

🤠 SPUR: Scaling Reward Learning from Human Demonstrations

Anonymous Author(s)

Affiliation

Address

email

1 **Abstract:** Learning reward functions from human demonstrations is criti-
2 cal for scalable robot learning, yet most approaches either require impractical
3 ground-truth state access, costly online retraining, or yield domain-specific mod-
4 els with poor transferability. We propose SPUR, a unified reward modeling
5 framework that combines a large pre-trained vision-language model (VLM) back-
6 bone fine-tuned to encode robot image sequences and language instructions, a
7 progress-based reward objective trained on successful demonstrations augmented
8 with video rewind to simulate failures, and a preference-learning objective over
9 mismatched and rewound trajectories to enable training on failed executions with-
10 out explicit progress labels. This design leverages the generalization of VLMs
11 while integrating complementary progress and preference signals for improved ro-
12 bustness and generalization. Experiments on out-of-distribution tasks in LIBERO
13 and Meta-World show that each component contributes to performance gains
14 across a set of reward metrics, and their combination achieves state-of-the-art
15 results compared to recent baselines, demonstrating scalable training of reward
16 models.

17 **Keywords:** CoRL, Robots, Learning

18 1 Introduction

19 An important problem in robot learning is that of learning rewards from human demonstrations [1]
20 to guide policy learning. When deploying robots in the real world, it's important that reward models
21 generalize to new tasks so that humans do not need to provide additional demonstrations, which is
22 expensive to scale, or train the reward models in tandem with the robot policies, which is sample-
23 inefficient and time-consuming. In this work, we investigate how to train reward functions that can
24 effectively generalize to new tasks without online training or additional demonstrations.

25 Prior works have attempted to develop generalizable reward functions, but they often assume access
26 to ground-truth states that may be difficult to provide in the real world [2, 3, 4, 5, 6, 7] or the ability
27 to train reward models from scratch in tandem with the policy [1, 8, 9], limiting their practical
28 applicability.

29 Some recent works instead propose reward models that can be directly used at test time, condi-
30 tioned solely on image observations and language instructions. One common approach is to leverage
31 the generalization capabilities of large vision-language models (VLMs) by querying them for *task*
32 *progress* to be used as reward [10, 11, 12, 13, 14], but these models have been shown to predict noisy
33 rewards difficult to be directly used for training robot policies [12, 13, 15]. Another is to directly
34 train a smaller reward model on human demonstrations. These methods use either a task-progress-
35 based training objective [16, 17, 15], or a preference-based or contrastive objective [18, 19, 20], but
36 they result in domain-specific reward models that are unlikely to generalize well to new domains.
37 Instead, we aim to train a generalizable reward model that can provide useful rewards, even on sig-

38 nificantly out-of-distribution tasks and settings. We hypothesize that ideas from all three threads of
39 work are useful, and combining them can lead to a reward model whose generalization is greater
40 than the sum of its parts.

41 To this end, we investigate how to blend together large-scale VLM backbones, progress-based
42 rewards, and preference-based rewards into one scalable, unified reward model we call SPUR
43 (**S**calable **P**rogress and **P**reference **U**nified **R44 pre-trained VLM backbone, not for zero-shot robot reward queries, but instead as a trainable back-
45 bone for encoding robot image sequences and language instruction tokens. SPUR then directly pre-
46 dicted task progress coming from successful demonstration trajectories, along with simulating failed
47 trajectories with *video rewind* augmentation [15], to produce useful per-timestep rewards for robots.
48 Finally, to help the model scale, SPUR also trains to predict binary *preferences* over mismatched
49 and rewound video sequences. This preference objective complements the reward prediction objec-
50 tive while also allowing for training with trajectories with *failed execution*, which progress-based
51 methods cannot train on without explicit progress labels for each failed trajectory.**

52 Through reward analysis experiments on new tasks in LIBERO [21] and Metaworld [22], we demon-
53 strate how each component complements the others for scalable training of generalizable reward
54 models. We also outperform recent, state of the art baselines across comparisons in both domains.

55 2 Related Works

56 2.1 Learning Reward Functions

57 Several prior works explored learning reward functions from various forms of supervision. One line
58 of research leverages direct human feedback, such as comparisons [23, 24, 25, 26, 27], rankings [28],
59 language annotations [9], and trajectory corrections [29, 30], to infer rewards. While these methods
60 can align reward functions with human intent, they typically require substantial human supervision
61 and are often sample-inefficient.

62 Another major direction is inverse RL (IRL), where reward functions are inferred from demon-
63 strations [1, 31, 32, 33] or implicitly from expert and goal-state distributions [34, 35, 36]. However, IRL
64 methods struggle to scale to high-dimensional state-action spaces and usually require new demon-
65 strations for every new task. In general, both human-feedback-based and IRL-based approaches
66 lack effective transfer mechanisms: when faced with a novel task, they often need to be retrained
67 from scratch. In contrast, our method leverages the semantic representations in VLM backbone to
68 transfer learned reward functions to unseen tasks without requiring additional human supervision.

69 2.2 Large Vision and Language Models as Reward Functions

70 Recently, LLMs and VLMs have been applied to reward design through code generation [5, 4, 37],
71 embedding-based reward estimation [38, 10], and preference-based feedback [8, 2]. However, most
72 of these methods assume access to privileged state information that is rarely available in real-world
73 settings. Another line of work employs VLMs as zero-shot success detectors, treating them as sparse
74 reward models [39, 40, 41]. While promising, this approach provides only episodic feedback and
75 misses the dense supervision signals present throughout the trajectory.

76 Some prior work explores task progress as a proxy reward, either by using VLMs as progress es-
77 timators [10, 11, 12, 13, 14] or by training task-specific models with progress-prediction objec-
78 tives [16, 17, 15]. VLM-based estimators, however, often yield noisy outputs, while smaller per-task
79 models tend to overfit to domain-specific dynamics, limiting their generalization to new domains.
80 In this work, we combine progress prediction with preference feedback over video sequences to
81 improve the reward learning objective. We further show that incorporating failure trajectory pairs
82 improves generalization across tasks

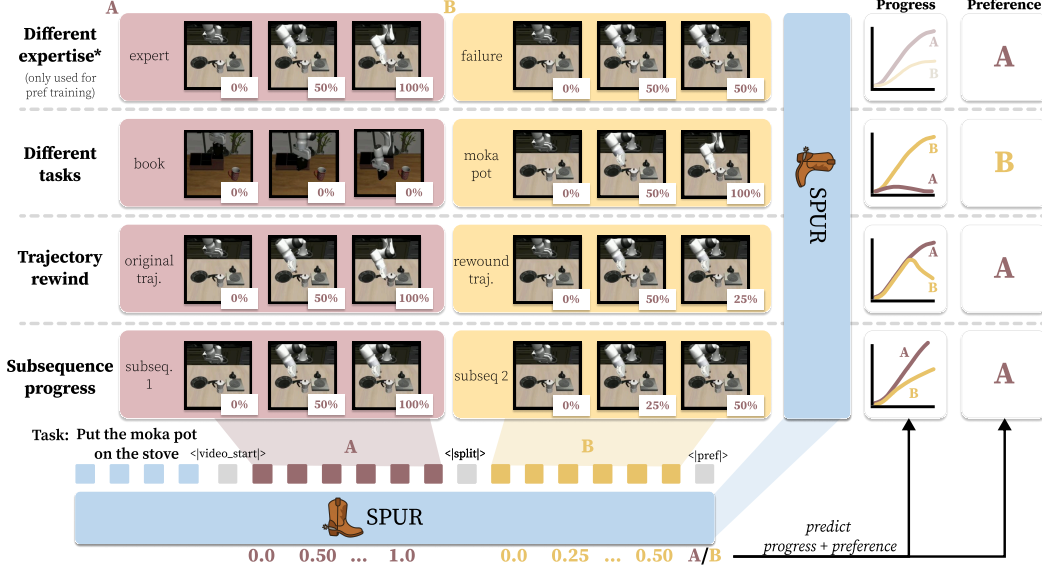


Figure 1: **SPUR**. Given two video trajectories, we train our VLM-based reward model, SPUR, to predict progress-based and preference-based rewards. We use four strategies (left) for curating training examples from our given datasets, which are further detailed in Section 3.2.

3 Method

We introduce SPUR, a generalizable reward model, as illustrated in Figure 1. We start with a dataset $\mathcal{D} = \{\tau_1, \tau_2, \tau_3, \dots\}$ consisting of robot demonstration trajectories $\tau = \{o_{1:T}, l, \text{success}\}$ with image observations o , language instructions l , and a success label $\text{success} \in \{0, 1\}$. To enable generalization to unseen tasks, environments, and domains, we first instantiate the reward model with a large-scale, pre-trained vision-language model (VLM) backbone. Then, we fine-tune it on two objectives that complement each other: predicting *preferences* over pairs of video trajectories and predicting continuous task *progress* as rewards.

3.1 VLM Base Model

Our base model is QWEN2.5-VL-INSTRUCT-3B [42], a 3B parameter, open-source, image and video-input VLM which demonstrates strong zero-shot performance across various vision and language tasks. SPUR can incorporate any base VLM model which supports language and video input, but we found QWEN to be easy to tune and performant. SPUR uses this model to take as input a natural language task description l and up to two different video sequences, $o_{1:T}^1$ and $o_{1:T}^2$ of arbitrary length. SPUR encodes both the language and videos as a single sequence of tokens with the base model’s tokenizer to construct its inputs as depicted below:

$$(l, o^1, o^2) \rightarrow \text{Token}(l) \langle|\text{video_start}|\rangle \text{Token}(o^1) \langle|\text{split_token}|\rangle \text{Token}(o^2) \langle|\text{pref_token}|\rangle, \quad (1)$$

where $\langle|\text{split_token}|\rangle$ is a special token that delineates the two video sequences. The VLM then produces a sequence of hidden states, which we use for preference and progress prediction, as detailed next.

3.2 Preference Prediction

To predict preferences, we attach an MLP head to the final hidden state corresponding to the special token $\langle|\text{pref_token}|\rangle$ from Equation (1) to produce preference logits. The model is trained to discern which of the two video sequences, $o_{1:T}^1$ or $o_{1:T}^2$, is better aligned with the given natural language task description, l . We denote the preference label as y , where $y = 1$ if o^1 is preferred over o^2 , and

107 $y = 0$ otherwise. Formally, the learned preference head MLP_{pref} produces a probability:

$$P(o^1 \succ o^2 \mid l) = \sigma(\text{MLP}_{\text{pref}}(h_{\langle|\text{pref_token}| \rangle})).$$

108 where σ is the sigmoid function and $h_{\langle|\text{pref_token}| \rangle}$ is the hidden state corresponding to the location of
 109 the $\langle|\text{pref_token}| \rangle$ in the input from Equation (1). The preference objective is optimized using the
 110 binary cross-entropy loss and backpropagated through MLP_{pref} and the VLM through $h_{\langle|\text{pref_token}| \rangle}$:

$$\mathcal{L}_{\text{preference}} = - \left[y \log P(o^1 \succ o^2 \mid l) + (1 - y) \log(1 - P(o^1 \succ o^2 \mid l)) \right].$$

111 **Preference Sample Construction.** Large-scale preference datasets comparing robot trajectories are
 112 not widely available, especially for training generalizable reward models. Given the scarcity of such
 113 data, we instead propose a suite of strategies for scalably curating a larger set of preference samples
 114 from existing trajectories without needing manual human annotations.

115 We construct preference pairs $(l, o^{\text{chosen}}, o^{\text{rejected}}, y)$ for training by sampling trajectories from \mathcal{D} ,
 116 always assigning o^{chosen} as the preferred observation sequence ($y = 1$). Given sampled trajectories
 117 $\tau = \{o_{1:T}, l, \text{success}\}$, we create batches of preference tuples sampled uniformly over the
 118 following four strategies:

- 119 **1. Different expertise.** Given a task instruction l , sample two trajectories $\tau_1, \tau_2 \sim \mathcal{D}$ with the
 120 same instruction where τ_1 has $\text{success} == 1$ and τ_2 has $\text{success} == 0$. We extract
 121 o^{chosen} from the observation sequence from τ_1 .
- 122 **2. Different tasks.** Sample a trajectory $o^{\text{chosen}} \sim \mathcal{D}$ corresponding to the task instruction l
 123 and a trajectory o^{rejected} with a different instruction. These samples encourage the model to
 124 ground correct video and language pairs.
- 125 **3. Trajectory rewind.** Following the idea proposed by ReWiND [15] that generated failed
 126 trajectories for reward *progress* prediction by *rewinding* videos, we propose to rewind suc-
 127 cessful videos to generate negative preference pairs. For a given trajectory $o^{\text{chosen}} = o_{1:T}$
 128 with $\text{success} == 1$, we first sample a random contiguous subsegment:

$$o_{\text{sub}} = o_{1:t_{\text{end}}}, \quad 1 \leq t_{\text{end}} \leq T.$$

129 We then generate a *rewound* trajectory o^{rejected} by reversing the last k frames of the o_{sub}
 130 where $k \sim \mathcal{U}(1, t_{\text{end}} - t_{\text{start}})$:

$$o^{\text{rejected}} = [o_{1:t_{\text{end}}}, o_{t_{\text{end}}-1:t_{\text{end}}-k+1}],$$

131 where $[.]$ denotes concatenating the videos. This procedure ensures that o^{chosen} represents
 132 the full progress along the subsegment, while o^{rejected} exhibits backward progress at the end.

- 133 **4. Subsequence progress.** For the same trajectory τ with $\text{success} == 1$, sample two
 134 subsequences $o_{1:t_1}, o_{1:t_2}$ with $t_1 < t_2$. We assign $o^{\text{chosen}} = o_{1:t_2}$ as it is further along in the
 135 task.

136 In practice, for all of these samples, we also sample the first frame randomly from the first half of
 137 the trajectory so that in datasets where the robot’s starting position is consistent across trajectories,
 138 SPUR does not overfit to the robot’s starting position.

139 3.3 Task Progress Prediction

140 In addition to preference prediction, SPUR also predicts the per-frame *progress* for each video as it
 141 can more directly be used for rewarding policies downstream [15]. Given a video $o_{1:T}$ with language
 142 instruction l , SPUR predicts a continuous progress value $p \in [0, 1]$ indicating the fraction of the task
 143 completed at each frame. The tokenized prompt is the same as in Equation (1) except without the
 144 second video o^2 .

145 Specifically, a progress prediction MLP head, $\text{MLP}_{\text{progress}}$, is attached to the hidden states $h_{\langle |o_t| \rangle}$
 146 corresponding to each frame t , thereby producing per-frame progress predictions. We train SPUR on
 147 the same data as in Section 3.2, with the exception of “Different expertise” where failed trajectories
 148 are not used for progress training as they do not have a ground truth progress to use. For a given
 149 video from a sampled trajectory $o_{1:T}$ (which can also be a subsequence), the progress prediction loss
 150 is computed as the Mean Squared Error (MSE) between predicted and ground-truth progress values:

$$\mathcal{L}_{\text{progress}} = \begin{cases} \sum_{t=1}^T \left(\text{MLP}_{\text{progress}}(h_{\langle |o_t| \rangle}) - \underbrace{\frac{t}{T}}_{\text{ground truth progress}} \right)^2, & \text{if not rewound} \\ \sum_{t=1}^T \left(\underbrace{\text{MLP}_{\text{progress}}(h_{\langle |o_t| \rangle}) - 0}_{\text{0 progress for mismatched tasks}} \right)^2, & \text{if wrong task} \\ \sum_{t=1}^{t_{\text{end}}} \left(\text{MLP}_{\text{progress}}(h_{\langle |o_t| \rangle}) - \frac{t}{T} \right)^2 + \sum_{t=1}^k \left(\text{MLP}_{\text{progress}}(h_{\langle |o_t| \rangle}) - \frac{t_{\text{end}} - t}{T} \right)^2, & \text{if rewound.} \end{cases} \quad (2)$$

Loss for original trajectory until t_{end} Rewind video for k frames from $t_{\text{end}} - 1$

151 We compute progress losses only for `success` trajectories, ensuring that the model learns meaningful
 152 temporal progress where the task is at least partially completed.
 153 Overall, our final pretraining objective for SPUR is: $\mathcal{L}_{\text{preference}} + \mathcal{L}_{\text{progress}}$.

154 4 Experiments

155 Our experiments aim to study the efficacy of each component of SPUR and compare it against
 156 baseline across a wide array of reward metrics. To this end, we organize our experiments to answer
 157 the following experimental questions, in order:

158 **(Q1)** Which components of SPUR contribute the most to generalizable reward prediction?
 159 **(Q2)** How does SPUR compare against baselines across a variety of reward metrics in unseen
 160 tasks?

161 **Setup:** We conduct experiments using the **LIBERO-90** dataset from the Lifelong Robot Learning
 162 Suite [21]. This dataset provides a diverse set of household manipulation tasks with various levels of
 163 distribution shift. Models are trained on demonstrations for 90 tasks in LIBERO-90 and evaluated
 164 on four benchmark splits: **LIBERO-10**, **Object**, **Spatial**, and **Goal**, which measure generalization
 165 across different dimensions such as goal, object, and spatial configurations. The original benchmark
 166 includes 4500 trajectories (50 per task) rendered at 128x128; following Kim et al. [43], we replay
 167 and re-render them at 256x256 and discard trajectories that did not replay successfully. We also
 168 include a corresponding set of failed trajectories constructed by replaying demonstration trajectories
 169 with added Gaussian noise on the actions.

170 We additionally compare on **MetaWorld** [22], specifically the 20-task training split consisting of
 171 5 demonstrations each from Zhang et al. [15]. Correspondingly, we evaluate on the corresponding
 172 17-task evaluation dataset across a variety of metrics proposed in Zhang et al. [15] that were shown
 173 to be reflective of downstream policy performance.

174 We list all dataset sizes in Table 4.

175 **Baselines:** We compare SPUR against several strong reward learning baselines:

- 176 • **ReWiND** [15]: trains a transformer-based network with a direct progress prediction objective
 177 using frozen language and image encoders along with video rewinding to simulate failed policy
 178 rollouts.
- 179 • **Generative Value Learning (GVL)** [14]: prompts a pre-trained Gemini LLM [44] with shuffled
 180 video frames to predict task progress for subsampled frames across the video sequence. We also

Table 1: **LIBERO Ablation Analysis.** Comparison of ablations across preference and progress accuracy metrics across unseen tasks in LIBERO-10, Object, Spatial, and Goal after training on LIBERO-90. – indicates metrics that are not applicable to the given model.

Category	Metric	Base Model	w/o Pref.	w/o Progress	w/o Fail. Traj.	SPUR
Preference Accuracy	Failed Trajs. \uparrow	0.5	0.64	0.82	0.69	0.91
Progress Accuracy	MSE \downarrow Reward Alignment $\rho \uparrow$	–	0.04 0.73	– –	0.04 0.73	0.03 0.81

181 convert its progress predictions to preference predictions by comparing last-frame predicted task
182 progress between queried trajectories.

183 • **RL-VLM-F** [8]: prompts a pre-trained LLM to obtain preference-based feedback predictions. We
184 query Gemini for these preference predictions.

185 **4.1 Q1: Which Components of SPUR Contribute the Most?**

186 First, we ablate individual components of SPUR to measure the effect of each. For these experiments, we train exclusively on LIBERO-90 data (both success and failure) and evaluate on the
187 188 unseen LIBERO-10, Object, Spatial, and Goal datasets.

189 • **Base Model:** Uses the pre-trained QWEN-2.5-VL-INSTRUCT-3B model to produce preference
190 and progress predictions via direct text prompting.

191 • **w/o Preference:** Removes preference losses from the training objective. Preference accuracy is
192 computed by using final-frame progress comparisons instead.

193 • **w/o Progress:** Removes progress losses from the training objective.

194 • **w/o Failure Data:** Removes unsuccessful trajectories from the preference training objective.

195 **Reward Metrics.** We compute: **preference accuracy** when comparing paired successful and failed
196 trajectories, and **progress prediction accuracy** in terms of mean-squared-error (MSE) against the
197 ground-truth progress target of successful trajectories and in terms of reward *alignment* in terms of
198 spearman correlation (ρ), measuring how well the predicted progress is ordered with respect to the
199 ground truth progress ordering of successful demonstrations.

200 Results averaged across our 4 unseen task distributions are displayed in Table 1, where the base
201 model performs at random chance on predicting preferences. We found it almost always produced
202 deterministically increasing progress predictions, so we do not include progress accuracy metrics.
203 Meanwhile, removing preference predictions hurts the progress accuracy and reward alignment com-
204 pared to SPUR, and removing progress predictions hurts the preference accuracy relative to SPUR.
205 Removing failed trajectories also predictably hurts unseen failed trajectory preference accuracy.
206 Overall, we demonstrate that SPUR performs the best across all comparisons and that each compo-
207 nent we ablate complements each other to increase overall performance.

208 **4.2 Q2: Reward Function Analysis in Unseen Tasks**

Table 2: **LIBERO Metrics.** Baseline comparison across preference and progress accuracy metrics
across unseen tasks in LIBERO-10, Object, Spatial, and Goal after training on LIBERO-90.

Category	Metric	RL-VLM-F	GVL	SPUR
Preference Accuracy	Failed Trajs.	0.39	0.65	0.91
Progress Accuracy	MSE \downarrow Reward Alignment $\rho \uparrow$	– –	0.07 0.68	0.03 0.81

209 Now, we compare SPUR against reward model baselines across unseen tasks in both LIBERO and
210 Metaworld. We first list **LIBERO** comparisons in Table 2 to GVL and RL-VLM-F. All methods are

211 trained on the same LIBERO-90 datasets where applicable (GVL and RL-VLM-F instead prompt
 212 pre-trained, closed-source generative models). We can see that SPUR outperforms RL-VLM-F by
 213 **2.9x** and GVL by **1.4x** on preference accuracy. Additionally, it outperforms GVL with less than half
 214 the progress prediction MSE and **1.19x** improvement on reward alignment correlation.

Table 3: **Metaworld Reward Metrics.** Comparison of reward models in terms of reward alignment (ρ) on Metaworld. Baseline results taken from ReWiND [15].

Category	Metric	LIV-FT	RoboCLIP	VLC	GVL	ReWiND w/o OXE	ReWiND w/ OXE	SPUR
Reward Alignment	$\rho \uparrow$	0.55	-0.01	0.62	0.57	0.64	0.79	0.83

215 Next we compare **MetaWorld** performance against an additional set of baselines on the MetaWorld
 216 evaluation dataset from ReWiND [15]. For a more comprehensive comparison, we also include
 217 additional baselines listed in Zhang et al. [15], namely LIV-FT [16], VLC [19], and RoboCLIP [10],
 218 along with ReWiND trained with and without the Open X-Embodiment (OXE) Dataset [45] as
 219 proposed in Zhang et al. [15]. We refer readers to Zhang et al. [15] for additional details about
 220 these baselines. Results in Table 3 indicate that SPUR outperforms the best-performing model,
 221 beating ReWiND even when it’s trained with additional data from OXE, and beating ReWiND’s
 222 performance by **1.29x** when both models are trained on the same data (w/o OXE).

223 5 Conclusion

224 We studied the problem of learning reward functions that generalize to unseen tasks without relying
 225 on additional demonstrations or online training. To address these challenges, we introduced
 226 SPUR a unified reward learning framework that leverages a large-scale VLM backbone together
 227 with both progress-based and preference-based objectives. By combining per-timestep progress
 228 prediction with preference supervision over mismatched and rewound trajectories, SPUR learns
 229 from both successful and failed executions while producing denser and more transferable rewards.
 230 Our experiments on LIBERO and Metaworld show that each component of SPUR contributes to
 231 improved generalization, and that the full model consistently outperforms recent state-of-the-art
 232 baselines across diverse reward metrics.

233 Looking forward, we believe that scalable reward learning frameworks such as SPUR offer a
 234 promising path toward reducing reliance on costly demonstrations and enabling more robust robot
 235 policy training in real-world settings. Future directions include extending our framework to longer-
 236 horizon tasks, enabling cross-embodiment reward transfer including human videos, and evaluating
 237 deployment in real-robot experiments.

238 **References**

239 [1] A. Y. Ng and S. J. Russell. Algorithms for inverse reinforcement learning. In *International*
240 *Conference on Machine Learning (ICML)*, 2000.

241 [2] M. Kwon, S. M. Xie, K. Bullard, and D. Sadigh. Reward design with language models. In *International Conference on Learning Representations (ICLR)*, 2023.

243 [3] H. Hu and D. Sadigh. Language instructed reinforcement learning for human-ai coordination.
244 In *International Conference on Machine Learning (ICML)*, 2023.

245 [4] W. Yu, N. Gileadi, C. Fu, S. Kirmani, K.-H. Lee, M. Gonzalez Arenas, H.-T. Lewis Chiang,
246 T. Erez, L. Hasenclever, J. Humplik, B. Ichter, T. Xiao, P. Xu, A. Zeng, T. Zhang, N. Heess,
247 D. Sadigh, J. Tan, Y. Tassa, and F. Xia. Language to rewards for robotic skill synthesis. In
248 *Conference on Robot Learning (CoRL)*, 2023.

249 [5] Y. J. Ma, W. Liang, G. Wang, D.-A. Huang, O. Bastani, D. Jayaraman, Y. Zhu, L. Fan, and
250 A. Anandkumar. Eureka: Human-level reward design via coding large language models. In
251 *International Conference on Learning Representations (ICLR)*, 2024.

252 [6] Y. J. Ma, W. Liang, H. Wang, S. Wang, Y. Zhu, L. Fan, O. Bastani, and D. Jayaraman.
253 Dreureka: Language model guided sim-to-real transfer. In *Robotics: Science and Systems*
254 (*RSS*), 2024.

255 [7] W. Liang, S. Wang, H.-J. Wang, O. Bastani, D. Jayaraman, and Y. J. Ma. Environment curricu-
256 lum generation via large language models. In *Conference on Robot Learning (CoRL)*, 2024.

257 [8] Y. Wang, Z. Sun, J. Zhang, Z. Xian, E. Biyik, D. Held, and Z. Erickson. RL-vlm-f: Reinforce-
258 ment learning from vision language foundation model feedback. In *International Conference*
259 *on Machine Learning (ICML)*, 2024.

260 [9] Z. Yang, M. Jun, J. Tien, S. J. Russell, A. Dragan, and E. Biyik. Trajectory improvement
261 and reward learning from comparative language feedback. In *Conference on Robot Learning*
262 (*CoRL*), 2024.

263 [10] S. A. Sontakke, J. Zhang, S. Arnold, K. Pertsch, E. Biyik, D. Sadigh, C. Finn, and L. Itti.
264 Roboclip: One demonstration is enough to learn robot policies. In *NeurIPS*, 2023.

265 [11] Y. J. Ma, S. Sodhani, D. Jayaraman, O. Bastani, V. Kumar, and A. Zhang. Vip: Towards
266 universal visual reward and representation via value-implicit pre-training. In *International*
267 *Conference on Learning Representations (ICLR)*, 2023.

268 [12] A. Adeniji, A. Xie, C. Sferrazza, Y. Seo, S. James, and P. Abbeel. Language reward modulation
269 for pretraining reinforcement learning. In *In RLC Reinforcement Learning Beyond Rewards*
270 *Workshop 2024*, 2024. URL <https://arxiv.org/abs/2308.12270>.

271 [13] Y. Fu, H. Zhang, D. Wu, W. Xu, and B. Boulet. FuRL: Visual-language models as fuzzy
272 rewards for reinforcement learning. In *Internatonal Conference on Machine Learning*, 2024.

273 [14] Y. J. Ma, J. Hejna, A. Wahid, C. Fu, D. Shah, J. Liang, Z. Xu, S. Kirmani, P. Xu, D. Driess,
274 T. Xiao, J. Tompson, O. Bastani, D. Jayaraman, W. Yu, T. Zhang, D. Sadigh, and F. Xia.
275 Vision language models are in-context value learners. In *International Conference on Learning*
276 *Representations (ICLR)*, 2025.

277 [15] J. Zhang, Y. Luo, A. Anwar, S. A. Sontakke, J. J. Lim, J. Thomason, E. Biyik, and J. Zhang.
278 ReWiND: Language-guided rewards teach robot policies without new demonstrations. In
279 *9th Annual Conference on Robot Learning*, 2025. URL [https://openreview.net/](https://openreview.net/forum?id=XjjXLxfPou)
280 [forum?id=XjjXLxfPou](https://openreview.net/forum?id=XjjXLxfPou).

281 [16] Y. J. Ma, W. Liang, V. Som, V. Kumar, A. Zhang, O. Bastani, and D. Jayaraman. Liv:
282 Language-image representations and rewards for robotic control. In *International Conference*
283 *on Machine Learning (ICML)*, 2023.

284 [17] K.-H. Hung, P.-C. Lo, J.-F. Yeh, H.-Y. Hsu, Y.-T. Chen, and W. H. Hsu. VICtor: Learning hier-
285 archical vision-instruction correlation rewards for long-horizon manipulation. In *International*
286 *Conference on Learning Representations (ICLR)*, 2025.

287 [18] D. Yang, D. Tjia, J. Berg, D. Damen, P. Agrawal, and A. Gupta. Rank2reward: Learning
288 shaped reward functions from passive video. In *International Conference on Robotics and*
289 *Automation (ICRA)*, 2024.

290 [19] M. Alakuijala, R. McLean, I. Woungang, N. Farsad, S. Kaski, P. Marttinen, and K. Yuan.
291 Video-language critic: Transferable reward functions for language-conditioned robotics. In
292 *Transactions on Machine Learning Research (TMLR)*, 2025.

293 [20] C. Kim, M. Heo, D. Lee, H. Lee, J. Shin, J. J. Lim, and K. Lee. Subtask-aware visual reward
294 learning from segmented demonstrations. In *International Conference on Learning Represen-
295 tations (ICLR)*, 2025.

296 [21] B. Liu, Y. Zhu, C. Gao, Y. Feng, Q. Liu, Y. Zhu, and P. Stone. Libero: Benchmarking knowl-
297 edge transfer for lifelong robot learning. *arXiv preprint arXiv:2306.03310*, 2023.

298 [22] T. Yu, D. Quillen, Z. He, R. Julian, A. Narayan, H. Shively, A. Bellathur, K. Hausman, C. Finn,
299 and S. Levine. Meta-world: A benchmark and evaluation for multi-task and meta reinforce-
300 ment learning. In *Conference on Robot Learning (CoRL)*, 2019.

301 [23] P. F. Christiano, J. Leike, T. B. Brown, M. Martic, S. Legg, and D. Amodei. Deep reinforcement
302 learning from human preferences. In *NeurIPS*, 2017.

303 [24] D. Sadigh, A. D. Dragan, S. S. Sastry, and S. A. Seshia. Active preference-based learning of
304 reward functions. In *Robotics: Science and Systems (RSS)*, 2017.

305 [25] E. Biyik, N. Huynh, M. J. Kochenderfer, and D. Sadigh. Active preference-based gaussian
306 process regression for reward learning. In *Robotics: Science and Systems (RSS)*, 2020.

307 [26] K. Lee, L. Smith, and P. Abbeel. Pebble: Feedback-efficient interactive reinforcement learn-
308 ing via relabeling experience and unsupervised pre-training. In *International Conference on*
309 *Machine Learning (ICML)*, 2021.

310 [27] J. Hejna and D. Sadigh. Few-shot preference learning for human-in-the-loop rl. In *Conference*
311 *on Robot Learning (CoRL)*, 2022.

312 [28] V. Myers, E. Biyik, N. Anari, and D. Sadigh. Learning multimodal rewards from rankings. In
313 *Conference on Robot Learning (CoRL)*, 2021.

314 [29] Y. Korkmaz and E. Biyik. Mile: Model-based intervention learning. In *International Confer-
315 ence on Robotics and Automation (ICRA)*, 2025.

316 [30] A. Bajcsy, D. P. Losey, M. K. O’Malley, and A. D. Dragan. Learning from physical human
317 corrections, one feature at a time. In *International Conference on Human-Robot Interaction*
318 (*HRI*), 2018.

319 [31] P. Abbeel and A. Y. Ng. Apprenticeship learning via inverse reinforcement learning. In *Inter-
320 national Conference on Machine Learning (ICML)*, 2004.

321 [32] B. D. Ziebart, A. Maas, J. A. Bagnell, and A. K. Dey. Maximum entropy inverse reinforcement
322 learning. In *AAAI Conference on Artificial Intelligence*, 2008.

323 [33] C. Finn, S. Levine, and P. Abbeel. Guided cost learning: Deep inverse optimal control via
 324 policy optimization. In *International Conference on Machine Learning (ICML)*, 2016.

325 [34] J. Ho and S. Ermon. Generative adversarial imitation learning. In *NeurIPS*, 2016.

326 [35] J. Fu, K. Luo, and S. Levine. Learning robust rewards with adversarial inverse reinforcement
 327 learning. In *International Conference on Learning Representations (ICLR)*, 2018.

328 [36] J. Fu, A. Singh, D. Ghosh, L. Yang, and S. Levine. Variational inverse control with events: A
 329 general framework for data-driven reward definition. In S. Bengio, H. Wallach, H. Larochelle,
 330 K. Grauman, N. Cesa-Bianchi, and R. Garnett, editors, *NeurIPS*, 2018.

331 [37] T. Xie, S. Zhao, C. H. Wu, Y. Liu, Q. Luo, V. Zhong, Y. Yang, and T. Yu. Text2reward: Reward
 332 shaping with language models for reinforcement learning. In *International Conference on*
 333 *Learning Representations (ICLR)*, 2024.

334 [38] P. Mahmoudieh, D. Pathak, and T. Darrell. Zero-shot reward specification via grounded natural
 335 language. In *International Conference on Machine Learning (ICML)*, 2022.

336 [39] J. Rocamonde, V. Montesinos, E. Nava, E. Perez, and D. Lindner. Vision-language models are
 337 zero-shot reward models for reinforcement learning. In *International Conference on Learning*
 338 *Representations (ICLR)*, 2024.

339 [40] Y. Du, K. Konyushkova, M. Denil, A. Raju, J. Landon, F. Hill, N. de Freitas, and S. Cabi.
 340 Vision-language models as success detectors. In *Proceedings of The 2nd Conference on Life-*
 341 *long Learning Agents*, pages 120–136, 2023.

342 [41] L. Guan, Y. Zhou, D. Liu, Y. Zha, H. B. Amor, and S. Kambhampati. Task success is not
 343 enough: Investigating the use of video-language models as behavior critics for catching unde-
 344 sirable agent behaviors. In *Conference on Language Modeling*, 2024.

345 [42] S. Bai, K. Chen, X. Liu, J. Wang, W. Ge, S. Song, K. Dang, P. Wang, S. Wang, J. Tang, et al.
 346 Qwen2. 5-vl technical report. *arXiv preprint arXiv:2502.13923*, 2025.

347 [43] M. J. Kim, K. Pertsch, S. Karamcheti, T. Xiao, A. Balakrishna, S. Nair, R. Rafailov, E. P. Foster,
 348 P. R. Sanketi, Q. Vuong, T. Kollar, B. Burchfiel, R. Tedrake, D. Sadigh, S. Levine, P. Liang,
 349 and C. Finn. OpenVLA: An open-source vision-language-action model. In *Conference on*
 350 *Robot Learning (CoRL)*, 2024.

351 [44] G. Team. Gemini: A family of highly capable multimodal models. *arXiv preprint*
 352 *arXiv:2312.11805*, 2024.

353 [45] O. X.-E. Collaboration, A. O'Neill, A. Rehman, A. Gupta, A. Maddukuri, A. Gupta,
 354 A. Padalkar, A. Lee, A. Pooley, A. Gupta, A. Mandlikar, A. Jain, A. Tung, A. Bewley, A. Her-
 355 zog, A. Irpan, A. Khazatsky, A. Rai, A. Gupta, A. Wang, A. Kolobov, A. Singh, A. Garg,
 356 A. Kembhavi, A. Xie, A. Brohan, A. Raffin, A. Sharma, A. Yavary, A. Jain, A. Balakrishna,
 357 A. Wahid, B. Burgess-Limerick, B. Kim, B. Schölkopf, B. Wulfe, B. Ichter, C. Lu, C. Xu,
 358 C. Le, C. Finn, C. Wang, C. Xu, C. Chi, C. Huang, C. Chan, C. Agia, C. Pan, C. Fu, C. Devin,
 359 D. Xu, D. Morton, D. Driess, D. Chen, D. Pathak, D. Shah, D. Büchler, D. Jayaraman,
 360 D. Kalashnikov, D. Sadigh, E. Johns, E. Foster, F. Liu, F. Ceola, F. Xia, F. Zhao, F. V. Fru-
 361 jeri, F. Stulp, G. Zhou, G. S. Sukhatme, G. Salhotra, G. Yan, G. Feng, G. Schiavi, G. Berseth,
 362 G. Kahn, G. Yang, G. Wang, H. Su, H.-S. Fang, H. Shi, H. Bao, H. B. Amor, H. I. Christensen,
 363 H. Furuta, H. Bharadhwaj, H. Walke, H. Fang, H. Ha, I. Mordatch, I. Radosavovic, I. Leal,
 364 J. Liang, J. Abou-Chakra, J. Kim, J. Drake, J. Peters, J. Schneider, J. Hsu, J. Vakil, J. Bohg,
 365 J. Bingham, J. Wu, J. Gao, J. Hu, J. Wu, J. Sun, J. Luo, J. Gu, J. Tan, J. Oh, J. Wu, J. Lu,
 366 J. Yang, J. Malik, J. Silvério, J. Hejna, J. Booher, J. Tompson, J. Yang, J. Salvador, J. J. Lim,
 367 J. Han, K. Wang, K. Rao, K. Pertsch, K. Hausman, K. Go, K. Gopalakrishnan, K. Goldberg,
 368 K. Byrne, K. Oslund, K. Kawaharazuka, K. Black, K. Lin, K. Zhang, K. Ehsani, K. Lekkala,

369 K. Ellis, K. Rana, K. Srinivasan, K. Fang, K. P. Singh, K.-H. Zeng, K. Hatch, K. Hsu, L. Itti,
 370 L. Y. Chen, L. Pinto, L. Fei-Fei, L. Tan, L. J. Fan, L. Ott, L. Lee, L. Weihs, M. Chen, M. Lepert,
 371 M. Memmel, M. Tomizuka, M. Itkina, M. G. Castro, M. Spero, M. Du, M. Ahn, M. C. Yip,
 372 M. Zhang, M. Ding, M. Heo, M. K. Srirama, M. Sharma, M. J. Kim, N. Kanazawa, N. Hansen,
 373 N. Heess, N. J. Joshi, N. Suenderhauf, N. Liu, N. D. Palo, N. M. M. Shafullah, O. Mees,
 374 O. Kroemer, O. Bastani, P. R. Sanketi, P. T. Miller, P. Yin, P. Wohlhart, P. Xu, P. D. Fagan,
 375 P. Mitrano, P. Sermanet, P. Abbeel, P. Sundaresan, Q. Chen, Q. Vuong, R. Rafailov, R. Tian,
 376 R. Doshi, R. Mart'in-Mart'in, R. Baijal, R. Scalise, R. Hendrix, R. Lin, R. Qian, R. Zhang,
 377 R. Mendonca, R. Shah, R. Hoque, R. Julian, S. Bustamante, S. Kirmani, S. Levine, S. Lin,
 378 S. Moore, S. Bahl, S. Dass, S. Sonawani, S. Tulsiani, S. Song, S. Xu, S. Haldar, S. Karamcheti,
 379 S. Adebola, S. Guist, S. Nasiriany, S. Schaal, S. Welker, S. Tian, S. Ramamoorthy, S. Dasari,
 380 S. Belkhale, S. Park, S. Nair, S. Mirchandani, T. Osa, T. Gupta, T. Harada, T. Matsushima,
 381 T. Xiao, T. Kollar, T. Yu, T. Ding, T. Davchev, T. Z. Zhao, T. Armstrong, T. Darrell, T. Chung,
 382 V. Jain, V. Kumar, V. Vanhoucke, W. Zhan, W. Zhou, W. Burgard, X. Chen, X. Chen, X. Wang,
 383 X. Zhu, X. Geng, X. Liu, X. Liangwei, X. Li, Y. Pang, Y. Lu, Y. J. Ma, Y. Kim, Y. Chebotar,
 384 Y. Zhou, Y. Zhu, Y. Wu, Y. Xu, Y. Wang, Y. Bisk, Y. Dou, Y. Cho, Y. Lee, Y. Cui, Y. Cao, Y.-H.
 385 Wu, Y. Tang, Y. Zhu, Y. Zhang, Y. Jiang, Y. Li, Y. Li, Y. Iwasawa, Y. Matsuo, Z. Ma, Z. Xu,
 386 Z. J. Cui, Z. Zhang, Z. Fu, and Z. Lin. Open X-Embodiment: Robotic learning datasets and
 387 RT-X models. In *International Conference on Robotics and Automation (ICRA)*, 2024.
 388

Table 4: Dataset

Dataset Splits	
Dataset	Num Trajectories
LIBERO90	3950
LIBERO10	388
LIBERO-Goal	432
LIBERO-Spatial	433
LIBERO-Object	456
LIBERO90 Failure	4312
LIBERO10 Failure	498
MetaWorld Train	100
MetaWorld Eval	85

Table 5: Configuration Parameters for SPUR Training

Training Configuration for RFM	
Parameter	Value
Base Model	Qwen/Qwen2.5-VL-3B-Instruct
Max frames (downsampled)	16
Per device training batch size	16
Learning rate	2e-5
Training steps	5000
Max sequence length	1024
LR scheduler	Cosine
Warmup ratio	0.1
Expertise / Task / Rewind / Subsequence ratio	[0.3, 0.3, 0.4, 0.0]